Numerical assessment of seawater intrusion in the Tripoli region, Libya

Saleh Ali Sadeg · Nurkan Karahanoğlu

Abstract Libya has experienced progressive seawater intrusion in the coastal aquifers since 1930s because of its ever increasing water demand from underground water resources. Tripoli City and its hinterland are located in the coastal region of the Gefara Plain, where the agricultural activity entirely depends on rainfall and groundwater. In recent years, the risk of seawater intrusion is continuously threatening coastal parts of the Gefara Plain that form one of the economically most significant area in the country. Hydrogeochemistry of the aquifer system was studied and a numerical assessment of the problem has been accomplished applying a two-stage finite element simulation algorithm. First, an areal, two-dimensional model was formulated in order to perform a steady-state calibration for the physical parameters, and boundary conditions of the hydrodynamic system. In the second stage, the mechanism of the seawater intrusion was analyzed using a cross-sectional finite element model. Simulation runs have been accomplished to study location of the interface and its temporal migration. The groundwater resource in the Tripoli region has been progressively contaminated by seawater intrusion. Simulation results indicate that the proposed scheme successfully simulates the intrusion mechanism. The seawater/freshwater interface would migrate landward leading to a very critical problem if the present groundwater production policy continues operating in the area.

Keywords Finite element simulation · Libya · Seawater intrusion · Tripoli

Received: 9 March 1999 / Accepted: 18 January 2001
Published online: 13 April 2001

S.A. Sadeg · N. Karahanoğlu (✉)
Department of Geological Engineering,
Middle East Technical University, 06531 Ankara, Turkey
E-mail: nurkan@metu.edu.tr

Introduction

Libya is one of the south Mediterranean countries and has a shoreline extent of about 1,900 km. Most of the population lives in the coastal cities of Tripoli and Benghazi. The Gefara Plain in the northwest of the country and the Jabel Al Akhder in the northeast, form fertile lands that contain more than 80% of the total agricultural activity (Fig. 1). The Gefara Plain, located between the Mediterranean coast and the Jabel Nafusa Mountain in the south, is also an industrial center for oil-related activities in Libya.

Groundwater is the main source for potable, industrial and irrigation water in Libya because of its semi-desert climate. Inevitably, groundwater extraction has been in excess of replenishment because of a rapid increase in agricultural and economic activities in the last 25 years. This has resulted in water level declines and deterioration in quality, including invasion of seawater along the coastal regions. At present, the seawater intrusion covers an area of $\sim$250 km^2 and the contamination front has already invaded 10 km inland in the Tripoli region.

Starting with the very well-known Ghyben–Herzberg relationship, seawater intrusion into coastal aquifers has been analytically and numerically investigated by several researchers (Bear and Dagan 1964; Shamir and Dagan 1971; Frind 1982; Wilson and Sa da Costa 1982; Reilly and Goodman 1985). Detailed research studies in this area have reported on increased seawater intrusion problems all over the world (Voss and Andersson 1993; Xue et al. 1993; Emekli et al. 1996). Recent efforts have been made to study the problem in very complicated aquifer conditions (Essaid 1990; Croucher and O'Sullivan 1995; Huyakorn et al. 1996).

The seawater intrusion problem in Libya has been the subject of several research papers. Cedestrom and Bastaiola (1960) are the first researchers who studied water resources in the Tripoli area. They detected saltwater intrusion effects on the groundwater resources near Salt Canal. Kruseman and Floegel (1978) also noticed the seawater intrusion and concluded that extracted groundwater was partially replaced by intruding seawater in the first few kilometers along the coast. Floegel (1979) conducted hydrochemical research along the coast of the Gefara Plain to define the intruding wedge and the diffused zones in the coastal region. He collected water

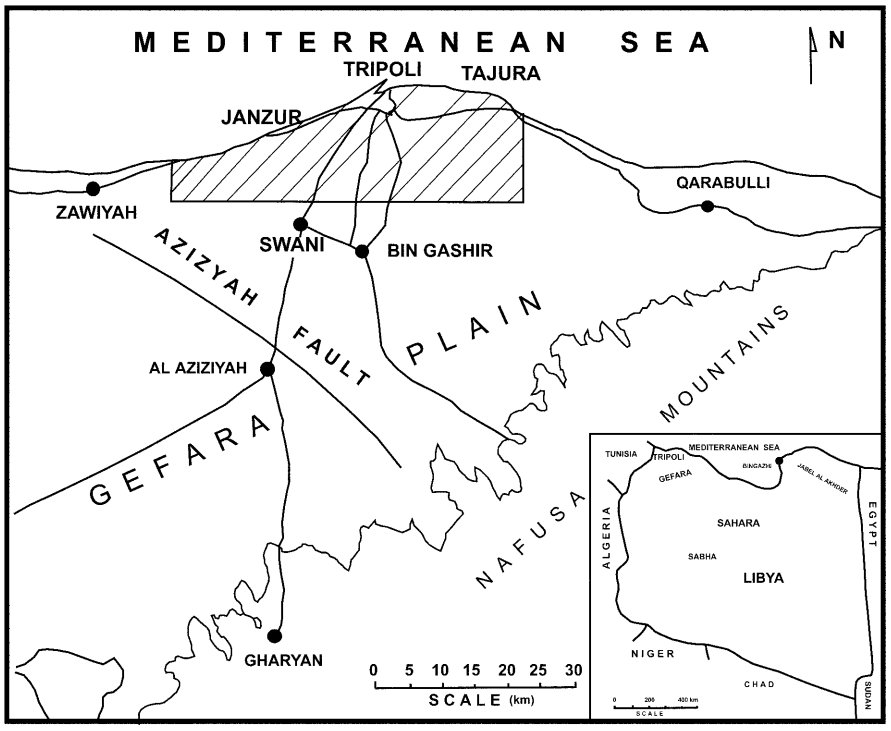

Fig. 1
Location map of the study area

samples from 14 N–S profiles. It is remarkable to note that five of these profiles were deliberately located in the Tripoli area, where the maximum contamination was observed at that time. Meludi and Werynski (1980) studied the seawater intrusion problem in Gargaresh–Swani Well Field, which has been a source of water supply to the Tripoli area since 1976. It was concluded that seawater intrusion into the area was progressing and that it was accelerated by the pumping of groundwater, especially at the well field. Bilal (1987) and Shawi and Philbert (1991) carried out detailed investigations and selected their research areas closer to the City of Tripoli. Bilal (1987) studied the seawater intrusion in Zanzur area (10 km west of Tripoli City) using 23 wells for sampling. Shawi and Philbert (1991) did similar research in the Tajura area (10 km east of the Tripoli City), collecting 123 water samples from wells. The common conclusion was that increased water demands for social, agricultural, and industrial developments made the seawater intrusion extend further inland in the 1990s than in the 1980s.
In addition to these hydrochemical/analytical studies there have been some numerical studies that have investigated the problem of seawater intrusion in NW Libya. The next two studies focused their simulations on the whole Gefara Plain and tried to investigate the problem at that scale. Krummenacher (1982) introduced a digital simulation model as a part of Gefara Plain Water Management Plan Project. The model was based on the Thyson–Weber finite difference method for a two-dimensional version of Laplace's equation. Water quality simulations were incorporated into the model; however, hydrodynamic dispersion and molecular diffusion were ignored. The model was used to predict future groundwater levels and water quality distribution in the Gefara Plain; however, a more recent study (NCB and MM 1993) states that predictions of this model do not match 1990 field observations. Backush (1983) applied a three-dimensional Trescott model to simulate the flow mechanism in the central part of Gefara Plain. He tried different transient flow scenarios and proposed a well field to minimize the saltwater intrusion rate into the upper aquifer. He concluded that maximum drawdown occurs in the middle of the simulated area (central part of the Gefara Plain) and from this design, an optimum amount of freshwater may be pumped from the aquifer with minimum saltwater intrusion.
In view of the previous studies we initiated this research to investigate the seawater intrusion problem in NW Libya. It aimed to define the hydrodynamic and hydrogeochemical behavior of the intrusion in the region and to assess its outcomes by applying simulation models. As Tripoli is the largest groundwater consumer in Libya, Tripoli City and its hinterland was selected as the research area. In this way it was planned to clarify where most ongoing intrusion occurred and to investigate it at a finer scale. Such research would not only define the intrusion mechanism in the area and its close vicinity, but also predict its future behavior. In this respect, this research hopes to contribute to the clear definition of the coupled mechanism between fluid flow and salt water dispersion–advection in the Tripoli region; to simulate the transient behavior of the intrusion mechanism and, most important of all, it is hoped that it will supply valuable information to further optimize management strategies. In this research, it was assumed that there exists a transition zone between freshwater and seawater phases, and that advection and diffusion control the movement of the intrusion front throughout the coastal aquifers.

Geological setting

The study area is located in the northern coastal part of the Gefara Plain and forms an almost rectangular area (763 km^2) between the Mediterranean Sea and the cities of Swani and Bin Gashir in the south (Fig. 1). The Gefara Plain, including the study area, has been the subject of numerous geological studies (GEFLI 1972; IRC 1975; Kruseman 1977; Krummenacher 1982; NCB and MM 1993). A review is given below that summarizes the geological outline of the Gefara Plain as a whole. Detailed information about the geology of the area can be obtained from the cited literature.

The Gefara Plain is characterized by a flat topography, and lies between the Mediterranean coast and the Nafusa mountains in the south. The plain can be divided into three different parts: the coastal strip, the central part and the foot-hill strip. The plain is covered by Quaternary deposits with occasional outcrops of limestone hills belonging to the Azizia formation. Calcarenites, covered by coastal sandstones and brown silts, form the coastal strip. The central part is covered mainly by poorly consolidated eolian deposits mixed with brownish silts. The southern border of the central part interlocks with the foot-hill strip, which is made up of fluvial and proluvial coarser sediments. The topographic elevation rises gradually toward the south and reaches 200 m above mean sea level at the south end of the plain. Seasonal streams flow over the central part and drain the plateau and fan out before reaching the sea. Other streams have longer courses and deepen their channels over the plain surface to form wadis. Gefara plain consists of Late Tertiary to Quaternary strata resting on a faulted and tilted Mesozoic basement. The Azizia formation (Fig. 2) is present throughout the Gefara plain, especially in the western and north central parts. It consists of dolomitic limestone and limestone, and north of Azizia, the fault dips to a great depth and reaches 900 m in the coastal area. The Abu Shaybah formation, consisting of cross-bedded sandstone alternating with green and red bands of clay, overlies the Azizia formation and is widely distributed over the Gefara plain. The Kikla formation (Lower Cretaceous) overlies the Abu Shaybah formation in the northern area and contains light colored, cross-bedded, friable quartz sandstone and conglomerates with brown, yellow and red silt and clay intercalations. The Ain Tobi formation (Upper Cretaceous) consists of limestone and forms most of the Nafusa escarpment at the southern border of the Gefara plain. The Upper Tertiary–Quaternary series consists of argillaceous sandstone with anhydrite subdivided by clay lens and reaches its greatest thickness in the Tripoli area. The Miocene–Pliocene–Pleistocene complex forms the top most series in the northern part of the Gefara plain. This unit consists of fossiliferous detrital limestone and marl formations alternating with yellow clay and sand lenses. The total thickness varies from 40 to 150 m. The Quaternary deposits cover the major part of the Gefara Plain as well as the plateau surface. The Gefara formation consists mainly of fine materials: mostly silt and sand occasionally with gravel and caliche bands. In the study area, the Gargaresh formation forms steep cliffs along the shore of the Mediterranean Sea. This formation is made up of calcarenite, including shell fragments and minor sand grains, interbedded with silt lenses. The sand dunes and sheets that cover large areas in this region represent eolian deposits in the Gefara plain (IRC 1975; Kruseman 1977; Krummenacher 1982).

Hydrogeology

The geology of the area includes a number of aquifers in the Gefara plain. They are separated by more or less impermeable clay lenses in the north; however they define a single large unconfined aquifer in the inland portion of the plain. The aquifers are described below to complete the information about the hydrogeology in Gefara Plain.

The upper aquifer (Miocene–Pliocene–Pleistocene) collects water under unconfined conditions and extends through-

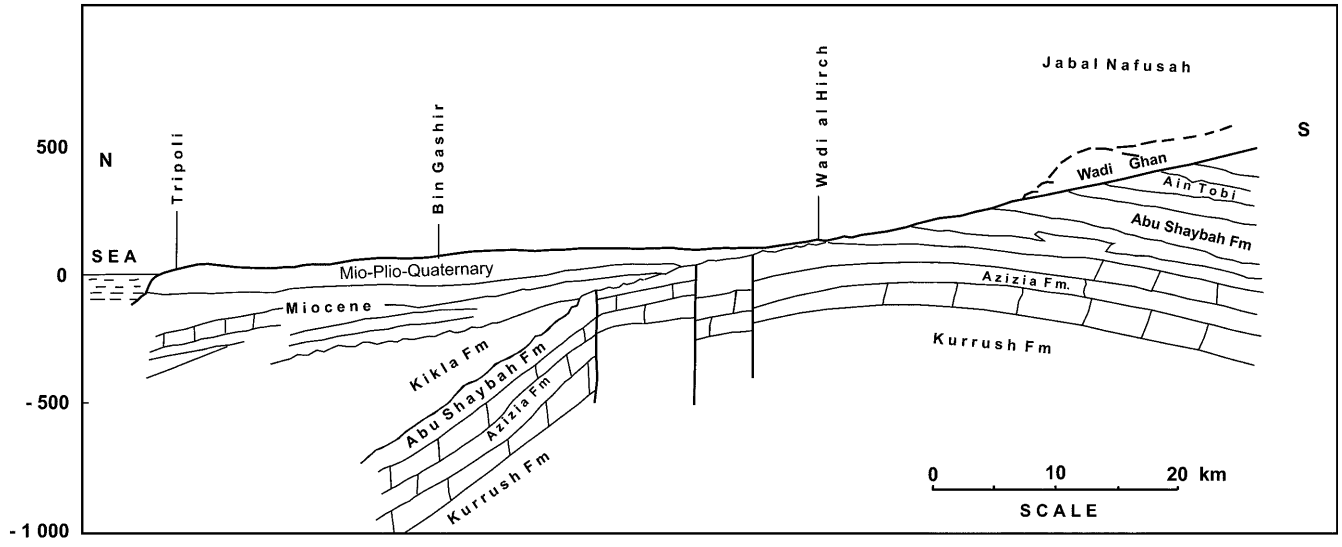

Fig. 2
A schematic cross section through the Gefara plain (Pallas 1978)

out the Gefara plain. It is 100–150 m thick and contains good quality water in the central and eastern parts. Along the coastal regions water quality becomes poor where overpumping has led to seawater intrusion. This aquifer forms the major source for domestic, industrial, and agricultural purposes for the Tripoli region. The Middle Miocene aquifer is well developed in the western part of the Gefara plain and it is found at 70–120 m below the surface. The thickness of the aquifer varies in from 125 to 200 m. Clay layers separate the aquifer from the Quaternary and Lower Miocene aquifers. The Lower Miocene aquifer consists of sandy limestone and overlies the sandy facies of the Upper Abu Shaybah formation. The Abu Shaybah sandstone aquifer is found in the northern parts, where the Abu Shaybah sandstone is overlain by Miocene units. The aquifer is thought to be hydraulically connected with the Lower Miocene aquifer. The Azizia limestone aquifer is found in the north of the Al Azizia fault and, because of its dip, the aquifer formation reaches a depth of 900 m in Ayn Zara (southeast of Tripoli). These aquifers show different transmissive and storage properties. Table 1 shows the aquifer system parameters as well as the average well yields and the total dissolved solid (TDS) values. The aquifer system in the Gefara Plain is thought to be mainly recharged from precipitation, infiltration from surface runoff, and by inflow from the south (Pallas 1978; Krummenacher 1982). In addition to these components NCB and MM (1993) consider the recharge by irrigation returns and by municipal supply losses. The main discharge of the groundwater from the aquifer system in the Gefara plain results from pumping for irrigation and domestic purposes.

Investigation of the water wells in the Tripoli region reveals that all of the wells pump water from the upper section of the Gefara Plain aquifer system. Considering this fact, the simulation study presented herein focuses on the upper aquifer (Quaternary–Miocene–Pliocene) of the Gefara Plain.

Seawater contamination in NW Libya

The Tripoli region in Libya has been exposed to problems of seawater intrusion since the construction of Salt Canal in the 1930s. Since then, rapid growth of population and an ever increasing water demand has accelerated progressive migration of seawater into the coastal aquifer. Cedestrom and Bastaiola (1960) noticed the early indications of seawater intrusion during their investigations in the area in 1957. They observed that some of the water wells near the coast started to be contaminated by seawater intrusion at that time (Fig. 3). GEFLI (1972) obtained a similar distribution for chloride concentration during an investigation in 1972 (Fig. 4). Comparison of these figures shows that there is a noticeable change in the position of isochlores, indicating landward migration of seawater.

In recent years, however, the intrusion effect is more remarkable. High rates of urbanization and increased agricultural and economic activities have required more water to be pumped from the aquifer. This pumping has continually increased the risk of seawater intrusion and deterioration of freshwater quality in the Gefara plain. Observations during a research project in 1994 showed that a 375 mg/l chlorine contour has migrated inland, reaching to distances of 10 km from the coast in Gargaresh and Ayn Zara regions (Fig. 5). A simple comparison of these figures clarifies that seawater contamination in the Gefara plain has been inevitably accelerated in recent years and that the problem will most likely become very crucial in the near future.

In order to make a proper definition of the intrusion, field research was undertaken and water samples were collected from water wells located along selected sea-to-land profiles. A network of 83 wells (47 irrigation and 36 domestic wells) was established to record water levels and to provide samples for chemical analysis (Fig. 6). The samples were analyzed for their physical (water levels, pH, and electrical conductivities) and chemical properties (major anions and cations), and they were interpreted together with the historic data to determine the deterioration level in the region and to form a background for further assessment studies. Table 2 shows a complete data set for the physical and the chemical properties of the water samples collected during the field research (in August 1994).

Water level recordings were interpreted to investigate temporal and spatial variation and the results are shown in Figs. 7, 8 and 9. Figures 7 and 8 depict areal changes of water levels in the 1957 and 1994 observation periods.

Table 1
Aquifer system parameters (after NCB and MM 1993)

Group	Formation	Well yield (m^3/h)	Transmission (m^2/day)	Storativity	TDS (mg/l)
Quaternary–Miocene	Gargaresh, Jefara, Qasr Al Haj	15–30	20–700	4–10%	500–2,000
Oligocene–Miocene	Al Khums	15–70	Up to 300	Confined	1,500–3,500
Cretaceous/Upper Jurassic	Sidi as Sid Kikla	40–90	Up to 520	Unconfined Mainly confined	1,000–1,500
Middle Jurassic	Tokbal	>15	Very variable	–	–
Triassic	Abu Shaybah	About 30	4–1,555	Confined	–
	Al Aziziyah	30–110	Up to 450	1–5% Confined	1,000–3,000
	Kurrush	2–10	About 60	Confined	2,000–10,000
	Ouled Chebbi	2–10	–	Confined	–

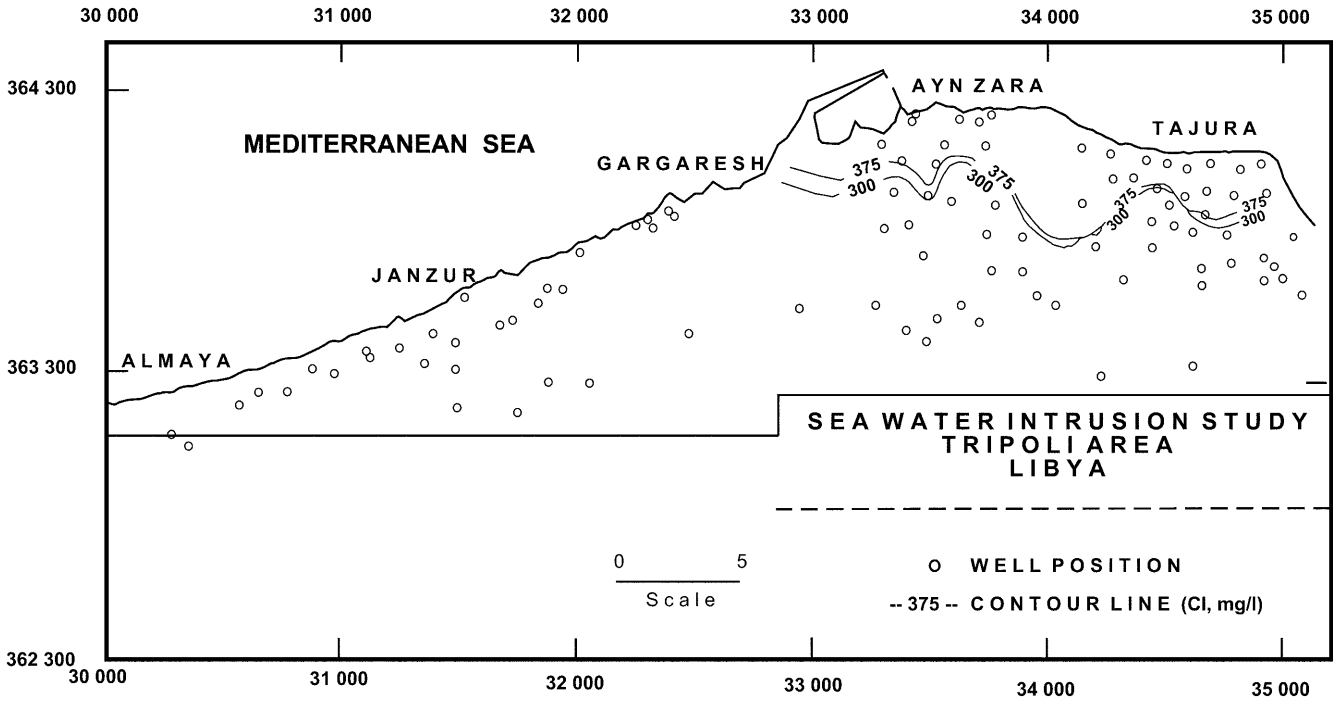

Fig. 3
Chloride concentrations in 1957 (after Cederstrom and Bastaiola 1960)

Water level contours have declined from south towards the north (Fig. 7), following smooth changes in a manner almost parallel to the coast line. This could well be thought of as the initial condition of the aquifer where only a few wells might pump water under steady-state conditions. In 1994, however, the situation was quite different and shows a great change in the contour lines. All over the area water levels have dropped and, along the southern boundary, drawdowns of more than 30 m are recorded. In addition to this, water levels often drop below sea level, presumably because of excessive discharge from a well field located in this profile. Comparison of the maps shows that the aquifer is over pumped because of increasing water demand in the region.

Figure 9 is constructed to show water level changes along the Gargaresh and Ayn Zara profiles. In both figures it is

Fig. 4
Chloride concentrations in 1972 (GEFLI 1972)

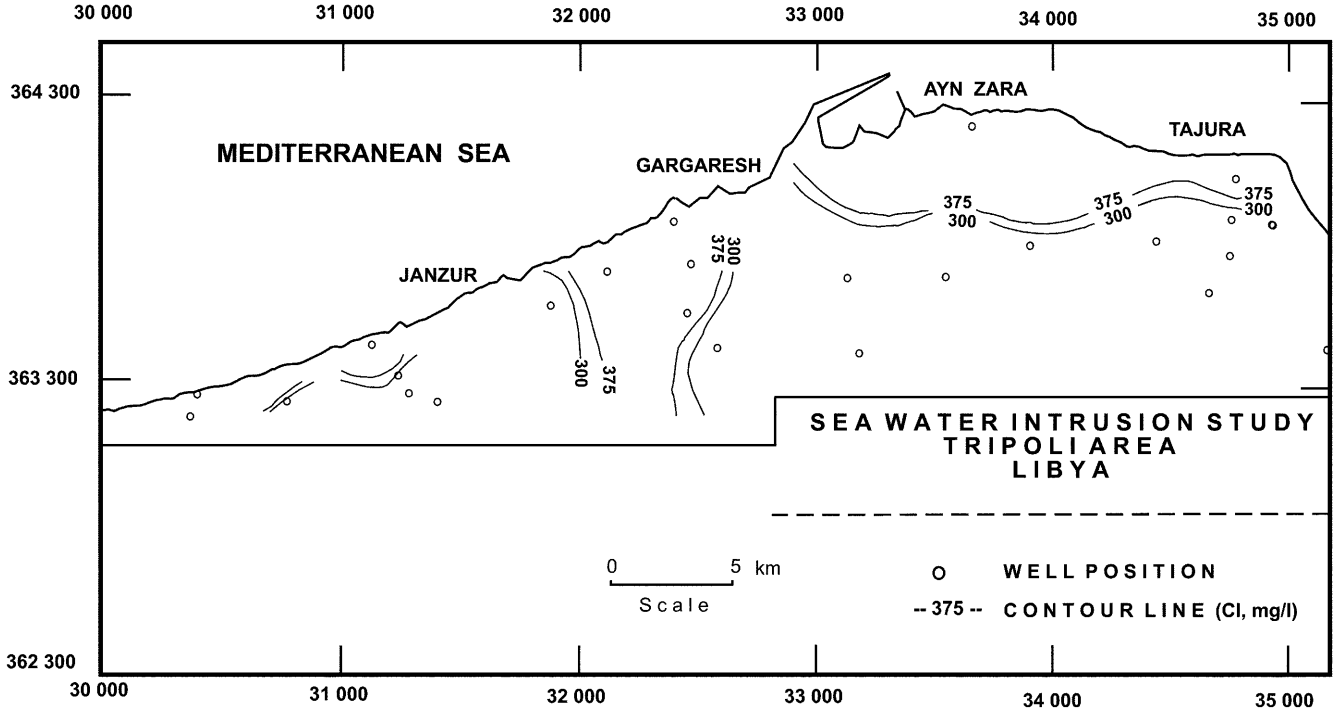

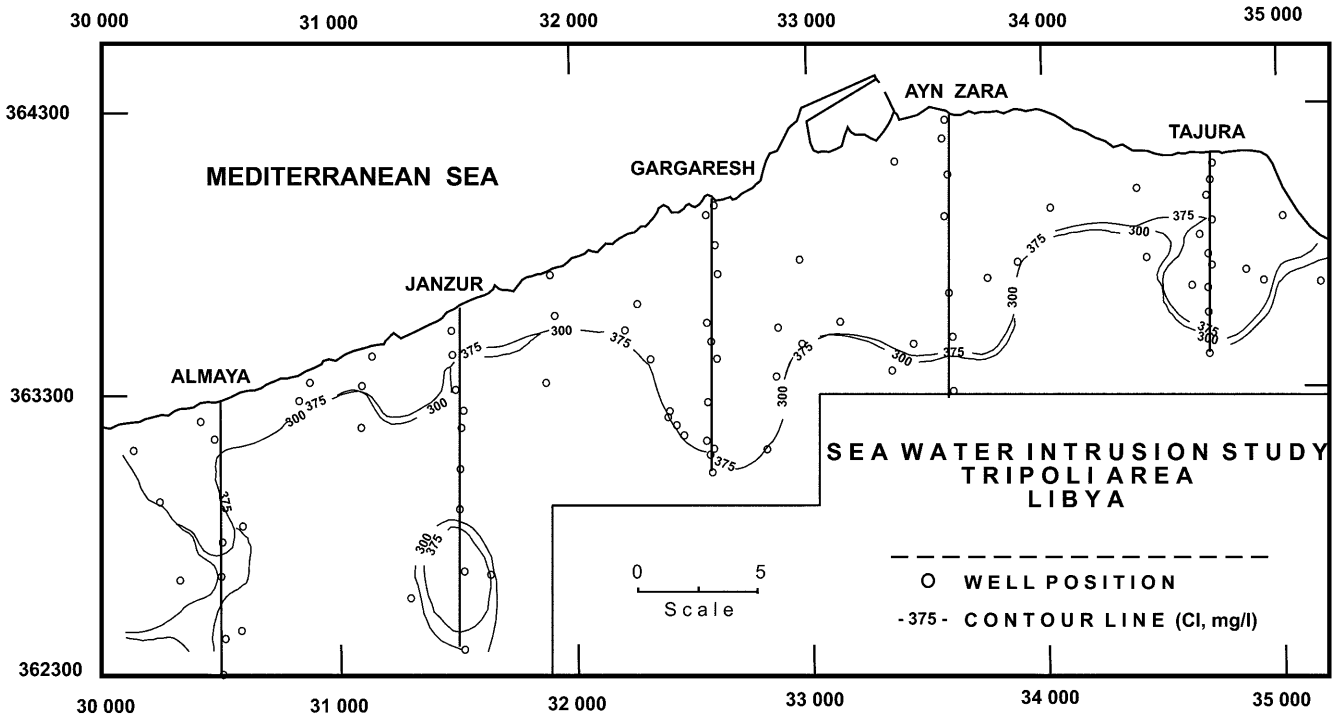

Fig. 5
Chloride concentrations in 1994

shown that water levels continuously decreased from 1957 to 1994. The excessive pumping from Swani Well Field resulted in a water level drop below sea level along the Gargaresh profile. Progressive declines in water levels follows the same trend in all sea-to-land profiles, indicating that the whole area has been continuously subjected to excessive water discharge.

Numerical simulation

The Mediterranean coast of Libya and the Gefara plain have been the subject of several researchers because of potential seawater contamination. FAO (1981) presented a groundwater model of the Gefara plain, where the Tyson–Weber finite difference method was applied. With this areal

Fig. 6
Sampling profiles and well locations

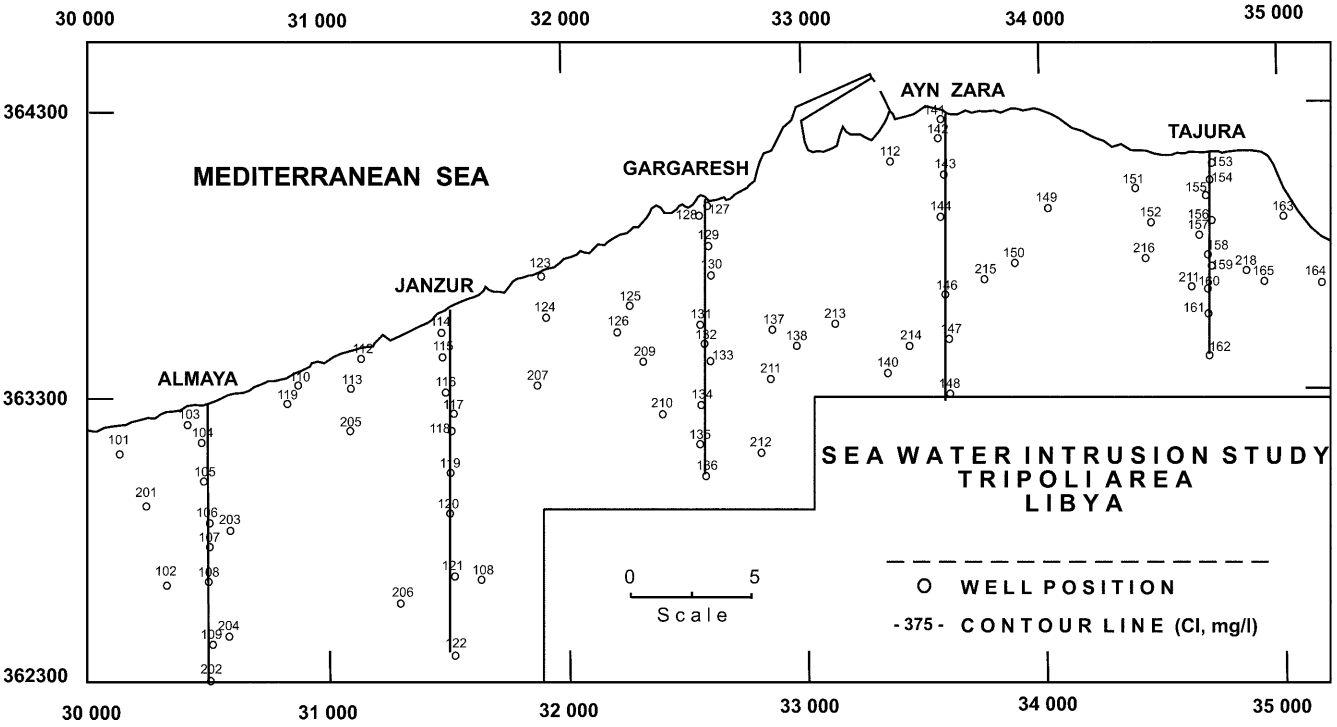

Table 2
The physical and the chemical properties of the water samples collected during August 1994 field research. Concentrations are listed in mg/l

Well no	pH	EC[a] (μmho/cm)	TDS	Cl	SO_4	HCO_3	Na	K	Ca	Mg	TH[b]	SAR
101	7.6	2,570	1,624	460	259	259	125	10	158	110	848	1.87
102	7.7	1,520	951	250	221	195	84.4	7.4	122	60	550	1.56
103	7.5	37,500	31,424	15,400	298	215	6,630	55.1	1,040	1,240	7,700	32.83
104	7.5	2,030	1,277	360	182	254	65.8	7.4	154	89	750	1.04
105	7.7	2,160	1,360	400	173	229	67.6	7.4	296	9	776	1.05
106	7.6	2,720	1,724	510	182	254	76.9	8.1	218	96	940	1.09
107	7.6	2,670	1,693	500	173	234	15.3	7.6	226	114	1,040	0.21
108	7.6	1,750	977	300	250	200	146	12	149	32	502	3.01
109	7.6	1,680	1,053	270	154	200	57.1	6.2	118	68	572	1.04
110	7.7	4,560	2,937	1,400	298	224	486	6.3	312	151	1,400	5.64
111	8.3	1,240	773	250	311	273	210	7.5	102	43	432	4.39
112	8.4	6,410	4,202	1,840	305	278	843	18	280	141	1,280	10.26
113	8.2	1,210	755	210	67	215	61.4	7.1	120	24	400	1.34
114	7.8	2,670	1,520	660	59	249	176	10.2	313	5	802	2.7
115	7.6	2,010	1,251	260	38	381	76.5	22.8	184	16	524	1.45
116	7.6	1,980	1,226	290	243	268	102	8.9	27	141	648	1.74
117	8.0	773	480	70	106	171	51	6.1	99	3	260	0.0
118	8.1	531	322	50	144	154	33.8	3	50	21	210	1.02
119	8.3	751	467	80	67	171	56	5.7	88	6	246	1.58
120	7.8	1,220	762	200	135	190	74.2	7.1	128	21	408	1.60
121	7.4	4,140	2,658	800	96	298	75.6	10.6	288	139	1,290	0.92
122	7.6	2,080	1,310	300	452	293	182	8.7	228	38	728	2.93
123	7.5	7,080	4,672	2,470	326	268	1,180	16.4	371	127	1,450	13.50
124	8.3	2,510	1,586	520	19	254	114	7.8	262	11	700	1.87
125	8.1	20,200	12,954	7,000	538	185	3,650	15.3	828	132	2,610	31.12
126	8.7	2,000	1,304	500	269	171	280	6.5	131	44	510	5.41
127	7.7	3,400	2,168	860	216	307	415	9.3	280	18	772	6.51
128	7.7	3,250	2,031	880	217	229	308	11.4	268	73	970	4.30
129	7.9	3,070	1,958	860	185	244	417	9.3	198	46	686	6.92
130	8.0	12,200	8,404	4,070	619	127	2,230	67.2	408	134	1,572	24.49
131	7.6	3,080	1,957	800	403	273	460	8.5	229	46	760	7.26
132	7.9	5,200	3,374	1,570	433	171	845	10.5	196	112	950	11.91
133	7.7	17,600	12,707	4,650	336	176	2,040	62.6	436	351	2,530	17.63
134	7.5	25,900	20,020	9,120	774	166	4,950	15.8	552	396	3,010	39.22
135	8.0	890	553	100	124	215	50.2	5.8	106	16	328	1.20
136	8.2	805	500	100	31	205	41.7	5.5	64	20	244	1.16
137	8.3	3,600	2,281	980	288	146	454	9.4	288	19	800	6.97
138	8.5	1,130	705	210	217	171	132	6.7	76	43	368	2.99
139	7.7	4,800	3,100	1,240	279	356	569	15.9	232	119	1,070	7.58
140	8.3	1,410	881	270	186	215	130	6.1	112	44	460	2.64
141	7.3	9,880	6,679	2,880	310	395	1,250	25.3	725	34	1,948	12.32
142	7.4	10,000	6,110	3,200	310	307	1,150	19.9	333	420	2,560	9.86
143	7.7	3,370	2,147	750	341	322	373	8.9	152	115	852	5.55
144	7.8	2,850	1,808	690	31	234	221	8.6	163	72	704	3.63
145	8.0	1,600	1,060	360	403	200	242	5.3	130	56	556	4.45
146	7.7	5,490	3,569	1,610	279	205	744	13.4	221	133	1,100	9.76
147	8.1	1,600	1,013	340	124	215	126	7.1	117	51	500	2.46
148	8.0	745	463	70	155	210	11.8	4.8	74	31	312	0.29
149	7.6	3,500	2,233	750	496	434	574	6.8	240	17	668	9.67
150	8.5	1,160	724	170	372	190	831	5.6	131	28	444	1.71
151	7.8	4,340	2,788	1,020	619	527	879	18.8	221	7	580	15.89
152	8.0	1,370	856	210	217	234	120	6.5	157	13	446	2.46
153	7.6	14,800	10,441	4,850	496	425	2,130	69.8	1,040	97	3,000	16.92
154	8.0	7,340	4,852	2,200	465	288	808	54	496	185	2,000	7.86
155	7.7	2,750	1,744	550	248	405	210	30.6	304	27	870	3.09
156	7.9	2,010	1,140	340	681	249	397	9.1	192	11	524	7.56
157	7.8	2,040	1,283	460	433	220	260	7.5	253	19	708	4.25
158	7.5	2,490	1,514	550	712	356	431	9.1	321	14	860	6.38
159	7.5	10,700	7,297	3,410	650	224	1,650	30.6	344	287	2,040	15.87
160	7.8	7,040	4,640	2,090	712	229	1,170	34.4	448	44	1,300	14.09
161	7.9	1,090	710	160	310	195	147	7	130	14	380	3.27
162	8.1	580	362	50	403	190	34	4.6	64	19	240	4.35
163	7.9	3,140	1,997	920	619	163	527	10.6	249	71	912	7.59
164	8.3	1,340	837	270	337	215	227	6.3	110	32	404	4.92
165	8.2	1,060	630	200	743	181	377	6.2	110	25	380	8.43

[a]EC is given at 25 °C
[b]Total hardness is in mg $CaCO_3$/l

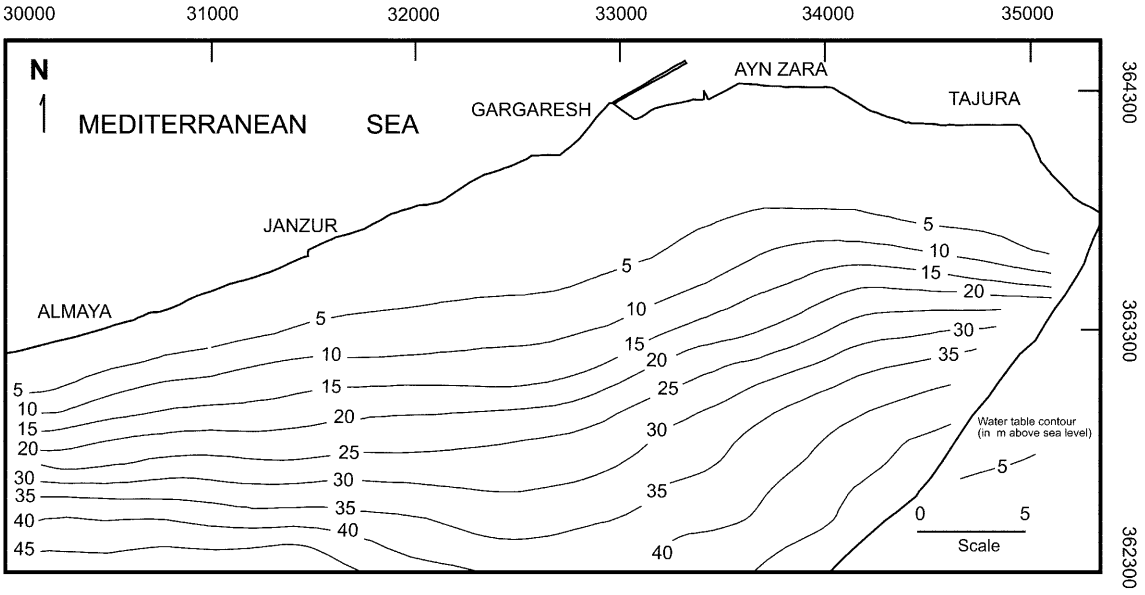

Fig. 7
Water table map for Tripoli area in 1957 (after Cedestrom and Bastaiola 1960)

simulation model the flow as well as the water quality was simulated, whereas the density variation was not incorporated into the model. Presumably because of this, it was found that model prediction of drawdown for 1990 overestimated the observed drawdown by 25 m (NCB and MM 1993). Backush (1983) applied a three-dimensional Trescott model to simulate the flow in the Gefara plain and studied the influence of different recharge and discharge conditions. NCB and MM (1993) applied an areal model to simulate both the flow and water quality variation in the Gefara plain. The model was used for steady-state and transient conditions until 1992 using annual time steps. Predictions were made for the groundwater levels and the quality variations under different recharge and discharge conditions. Careful inspection of the previous modeling studies reveals that all these models tried to simulate the overall Gefara plain. One of them applied a three-dimensional model to simulate only the flow mechanism; however, the others applied areal simulators for the water flow and water quality changes. It is important to point out that no effort has been made so far to investigate vertical gradients in the salt water content.

Considering these studies, a numerical model was formulated to simulate the drawdown and salt concentration distribution to clarify the intrusion mechanism in the Tripoli region, located in the northern part of the Gefara plain. In order to add a new perspective to the previous studies a quasi-three-dimensional modeling approach was applied, which gave an opportunity to couple the flow and diffusion mechanisms in the areal and vertical

Fig. 8
Water table map for Tripoli area in August 1994

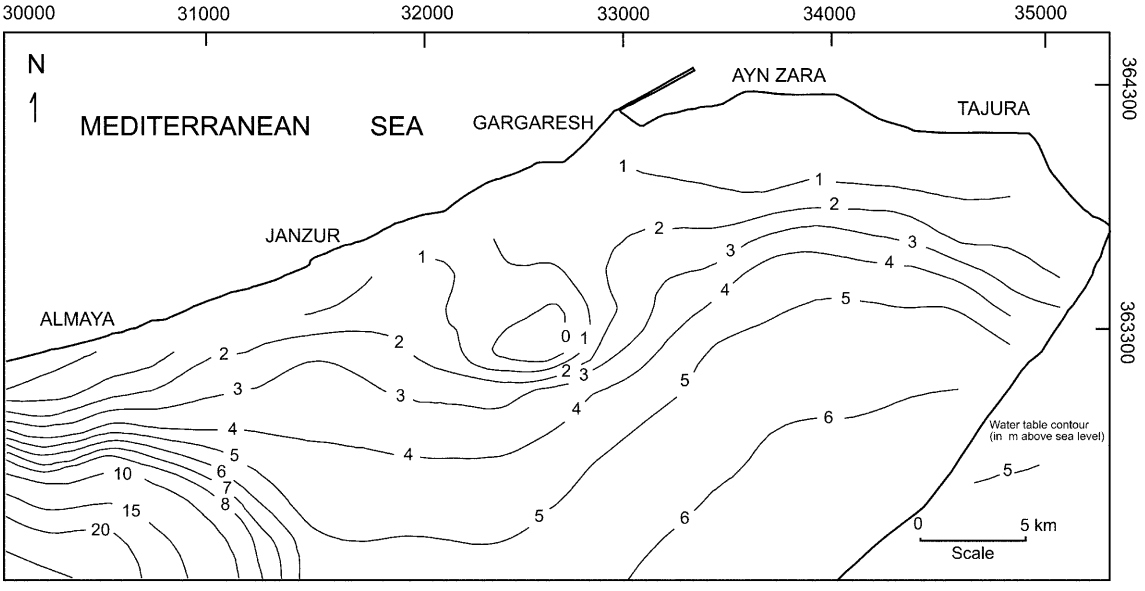

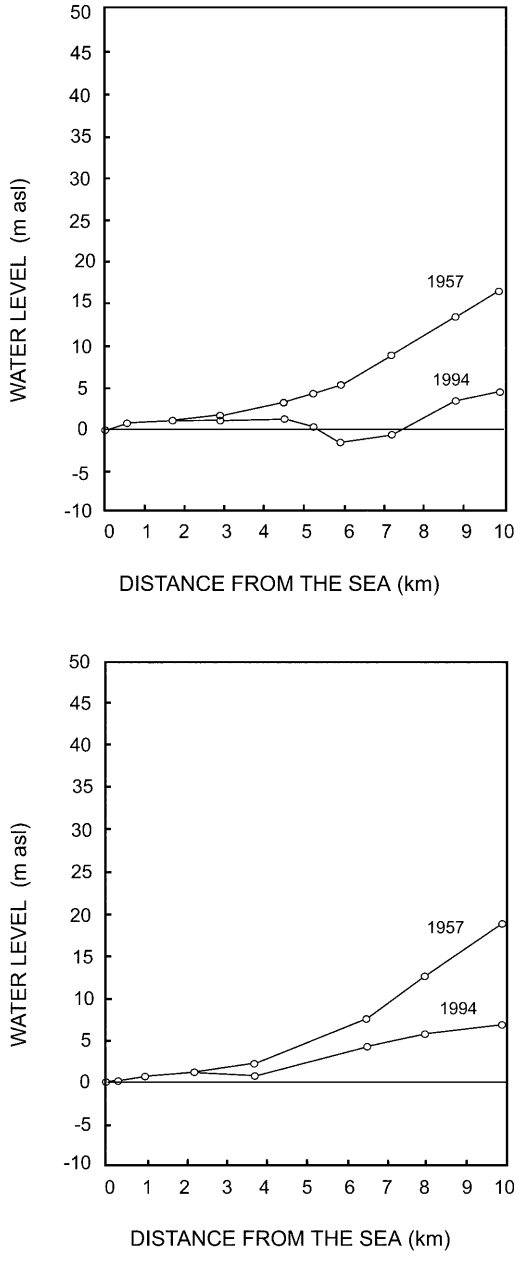

Fig. 9
Temporal change of water levels along Gargaresh and Ayn-Zara profiles

domains. In this way we hoped to determine both the areal distribution of the unknowns as well as their variations in a vertical section. The major objective of this research was to simulate the coupled mechanism and make future predictions for proposing optimal management strategies to reduce seawater intrusion.

The model was constructed to solve the ground water flow and salt diffusion equations assuming a dispersive type of equilibrium between saltwater and freshwater. The two-dimensional version of the SUTRA model (Voss 1984) was used in the study. Numerical assessment of the problem has been accomplished by the sequential use of two 2-D models. First, an areal depth integrated 2-D flow model was applied to calculate the head distribution in the region under steady-state conditions. During the steady-state calibration runs, the most suitable physical parameters (hydraulic conductivity, 1–30 m/days; see Fig. 10) and the boundary conditions of the hydrodynamic system were obtained. In doing so, western and northeastern boundaries were assumed to have no flow type, and the southern and northeastern boundaries continuously recharged the aquifer. The amount of recharge was computed using Darcy's equation with different values of hydraulic conductivity. The calibration runs continued until a good match was obtained between the observed and the computed heads (Fig. 11). In the second stage, these results were used as input data in a density-dependent cross sectional finite element model to simulate the coupled mechanism of seawater intrusion. Simulation runs were accomplished along a vertical cross section (Gargaresh profile) over the areal mesh to analyze the position of the interface and its temporal migration.

An areal flow model

Simulation analysis started with modeling the steady-state freshwater flow mechanism in the Tripoli region. Water level measurements in 1957 were considered as the initial steady-state conditions because they reflect the initial hydrodynamic conditions in the area. Figure 11 is constructed to show the steady-state groundwater table contours.

A (four-nodal) quadrilateral finite element mesh was constructed to perform the areal simulation task. During mesh discretization, correspondence between existing wells and the nodal points, boundaries of the aquifer and the present-day position of the intrusion were considered. The mesh covers an area of 763 km^2 (including the city of Tripoli) and contains 398 quadrilateral elements with 444 nodes (Fig. 10). The mesh was checked for its numerical stability and found to be appropriate for the simulation studies. The model was bounded by constant head (Dirichlet type), no-flow and recharge (Neumann type) types of boundary conditions. The nodal points along the Mediterranean coast were given constant heads with fixed values for the heads along this boundary. Western and northern parts of the eastern boundary were defined by analyzing the steady-state flow behavior in the aquifer. Figure 11 depicts a uniform steady-state flow from south to north in the aquifer forming flow lines that are nearly perpendicular to the coast. Considering this flow behavior, the western and northern parts of the eastern boundary were located on flow lines. This means that these boundaries were considered as no-flow type, which indicates that the flow can only take place along these boundaries, but not across them. The southern and southeastern boundaries of the aquifer were defined by recharge boundary condition, across which the aquifer was continuously recharged. Steady-state model calibration was accomplished by applying a trial-and-error procedure. The steady-state flow model was calibrated by suitably adjusting the hydraulic conductivities until a good match was obtained between

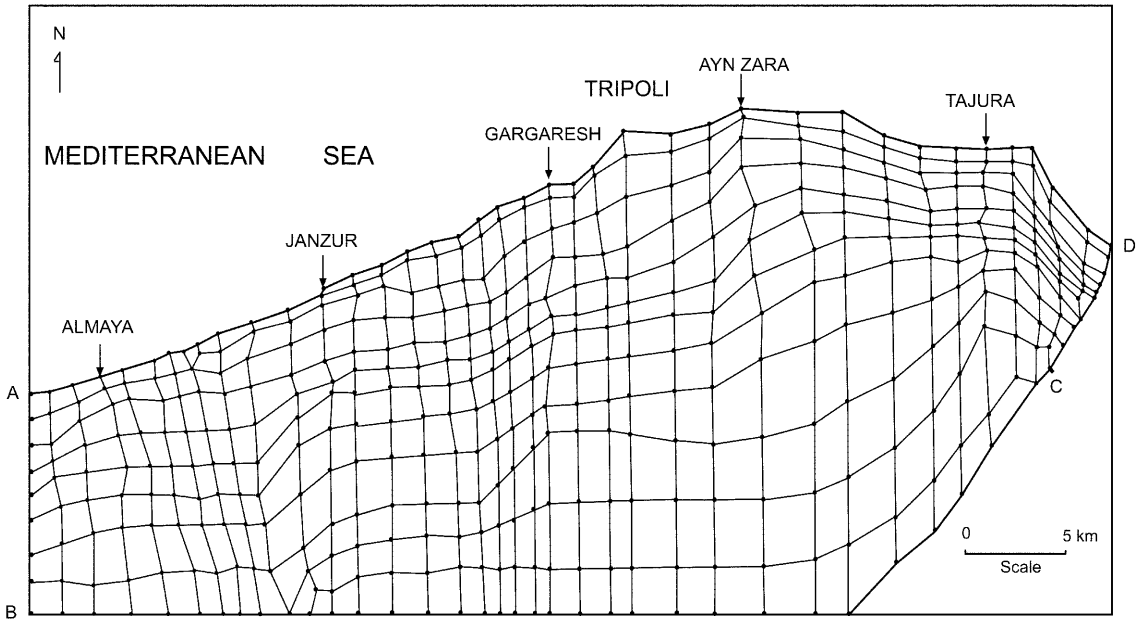

Fig. 10
Areal model finite element mesh and the boundary conditions

the computed and observed water levels. In doing this, we tried to minimize the sum of squared deviations in the computed and observed heads after each trial (Anderson and Woessner 1992). After several calibration runs the least value for the squared deviations was reached and it was decided that the calibration was complete. It was found that the calibrated water levels showed an average of 0.04 m deviation from the observed heads (Fig. 11). Good correlation between the computed and observed heads suggests that the model was successfully calibrated to the field conditions by using the boundary conditions and by suitably adjusting hydraulic conductivity values (Fig. 12). Sensitivity of the calibrated model was tested against hydraulic conductivity variations and it was found that the model was very sensitive to lower values of hydraulic conductivity (Fig. 13).

Fig. 11
Comparison of the observed (*solid lines*) and the computed water levels (*dashed lines*) after steady-state calibration

Cross sectional model

The second stage of the simulation algorithm was directed to investigate the coupled mechanism of fluid flow and salt

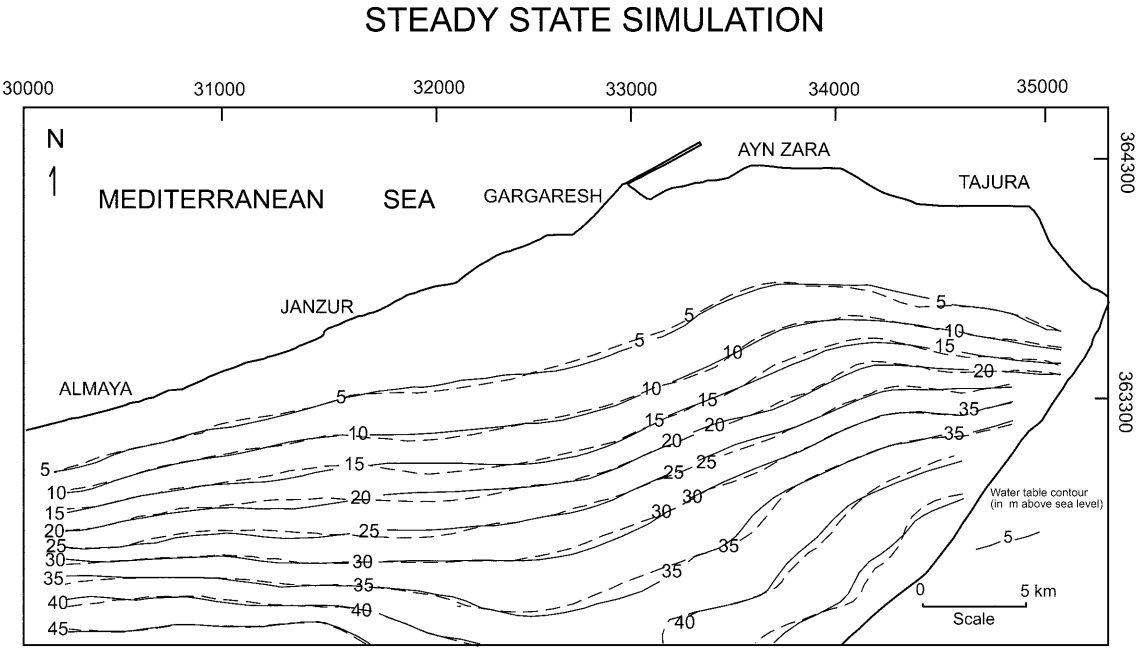

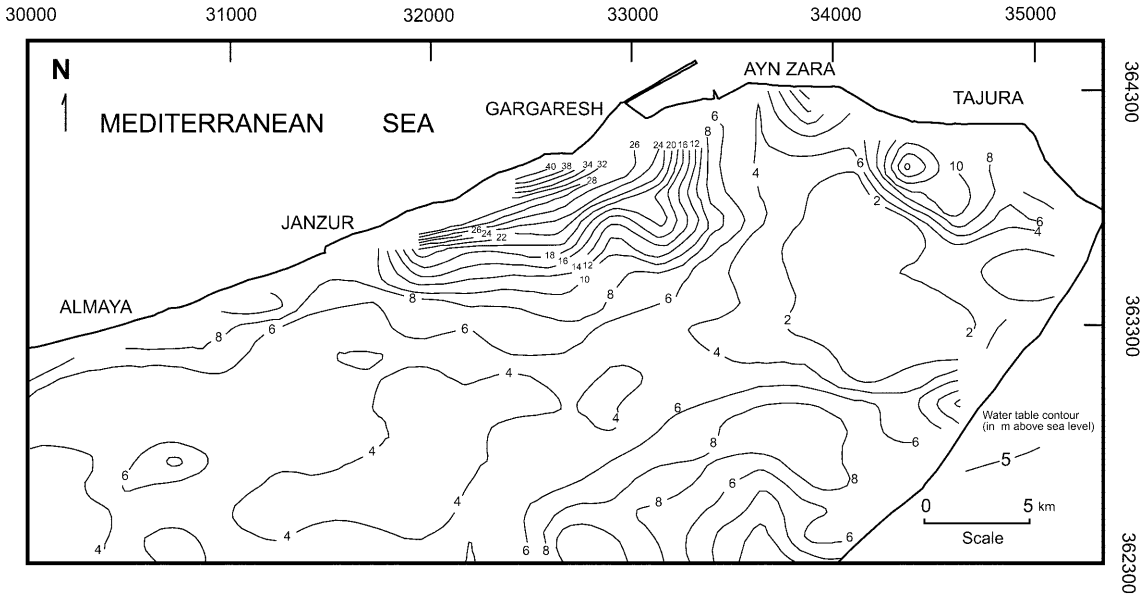

Fig. 12
Hydraulic conductivity distribution map

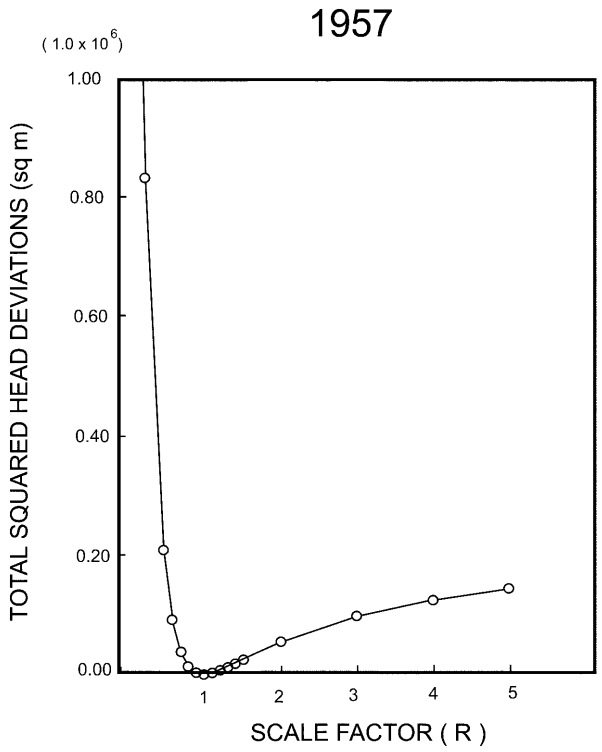

Fig. 13
Sensitivity analysis for the Calibrated areal model

transport in the aquifer system by means of a cross sectional model. Such an analysis also included the mechanism of salt movement by the density difference of fresh water and seawater. In fact, this mechanism is the major factor controlling natural separation of these phases, hence controlling the position of the interface under steady-state and transient conditions.

Cross sectional analysis involves stages of transient steady-state calibration, transient modeling and future predictions along the Gargaresh profile. In the first stage, a transient steady-state calibration was performed to determine the initial position of the interface through a temporal analysis. It was expected to approach a steady-state in this analysis with a series of time steps. At time zero, seawater begins to intrude into the aquifer (where there is no salt water initially) across the sea boundary. In this way, the initial position of the interface is approached by progressive intrusion of seawater. This mechanism is simulated by transient steady-state calibration and the transient solution is continued until a negligible difference is detected between successive time steps. Dispersive coefficients of the aquifer(longitudinal 25 m and transverse 1 m), the porosity (uniform porosity of 0.1 is used) and the initial concentration distribution within the cross section were determined in this calibration study. In the transient modeling stage (history matching), the transient response of the aquifer and the interface were simulated for the period between 1957 and 1994. Starting from the initial head and concentration distributions, the modeling was progressed through time to simulate the response of the aquifer to temporal changes in average recharge and discharge rates. In the last stage, the future behavior of the intrusion was predicted by using the present hydrodynamic conditions in the aquifer.

Considering its high water demand potential, a cross section along the Gargaresh profile was taken from the shore towards inland. The section passes through several nodes, including nine real-well nodes of the areal mesh, so that they could be used in defining the boundary and initial conditions. The section is 150 m thick and extends 17 km into the central part of the Gefara Plain, forming a boundary that was not affected by seawater intrusion.

A finite element mesh was discretized along the Gargaresh profile. The mesh consists of 630 quadrilateral elements

and 742 nodes (Fig. 14). There are 105 elements located horizontally with six layers in the vertical direction, reaching down to the bottom of the aquifer. The mesh has got finer elements in the region of the aquifer, where the transition zone is expected. Element sizes become coarser towards inland in the horizontal direction, keeping a fine element size of 25 m in the vertical direction.

After developing the mesh a transient steady-state calibration was conducted to calibrate the dispersivities and the porosity in 1957. Because operating wells are relatively few in number and they have different screen depths, and hence produce a mixture of waters, the available field data on concentrations were not adequate to define the position of the interface for successful field calibration. Therefore, it was decided to locate the interface and calibrate the model to the field conditions using a transient steady-state approach. In this approach, the governing equations were solved over a long period of time unless a transient equilibrium was reached between the fresh and the salt water phases within the aquifer. It was assumed that there was no salt water in the aquifer and, at time zero, salt water starts to intrude from the sea boundary and reaches an equilibrium gradually with time. The equilibrium position determines the location of the interface, which indicates that the flow and diffusion mechanisms reach their steady-state behavior. This procedure was also supported by the findings of Voss (1984), who stated that the intrusion problem was nonlinear and could be solved by approaching a steady-state with a series of time steps.

During calibration runs, the following initial and boundary conditions were used (Fig. 14). At the sea boundary, the nodes were given fixed 0-m heads and the inflowing water was assigned a concentration value of 0.0395 kg/l (completely seawater). At the inner-land boundary a recharge boundary condition was applied. Magnitude of the recharge, which was expected to keep the heads at 38.5 m, was calculated by considering areal model results. At this boundary inflowing water had a concentration value of zero. The lower boundary of the aquifer was defined by a "no-flow" type boundary condition and, initially, all the interior nodes were assigned zero concentrations. Hydraulic conductivity values were transferred from the areal model results. Density of seawater was taken as 1,027.83 kg/m3 and the density of fresh water was 1,000 kg/m^3. A uniform porosity value of 0.1 was used considering a previous study in the area (GEFLI 1972).

A transient steady-state calibration procedure was performed in four steps. First a time-step length analysis was conducted using zero dispersivities in the solutions. Time-step lengths of 1, 5, 10, 15, and 30 days were tried and it was observed that oscillatory solutions were obtained starting with a 10-day time-step. Therefore, a 5-day time interval was selected to be used as the optimum time-step

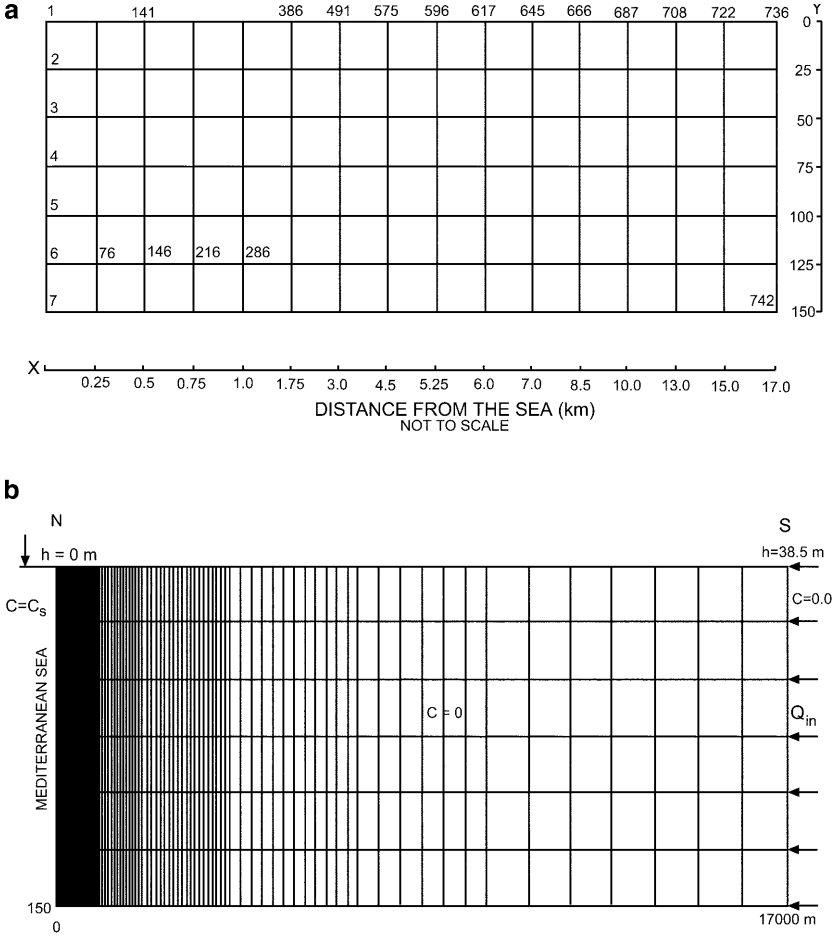

Fig. 14
a Some nodes in the cross sectional mesh; **b** cross-sectional mesh and the boundary conditions (not to scale)

length in the foregoing simulation runs. Next, the calibration process was repeated for different longitudinal (10, 20, 30, and 50 m) and transverse (0.1, 1, and 10 m) dispersivities. Solutions were found to be sensitive to these parameters, and non-oscillatory solutions for the heads and concentrations were obtained using 25 m for the longitudinal and 1 m for the transverse dispersivities. In the third stage, the modeling equations were solved for a long period of time using appropriate physical parameters, suitable time-step lengths and the boundary and initial conditions. Steady-state solutions were obtained by running the program for 2,000 days (400 time steps) when the percentage changes decreased down to 0.47% for concentrations and 0.005% for the heads (Fig. 15). In the last stage computed, values were compared with the field observations to calibrate the model to field conditions. Steady-state calibration of the model was based on the 1957 field observations of Cedestrom and Bastaiola (1960). Steady-state water level and concentration distributions are shown in Figs. 3 and 7. Considering these figures, calibration of the cross section model was made by comparing calculated heads with results of the areal model at the nodes along the Gargaresh profile. Computed and observed water levels at these nodes were plotted to show their close similarity (Fig. 16). A slight discrepancy along the seaward nodes is attributed to transfer of computed nodal pressures into nodal heads. It should also be noted that, during transfer of the areal hydraulic conductivities

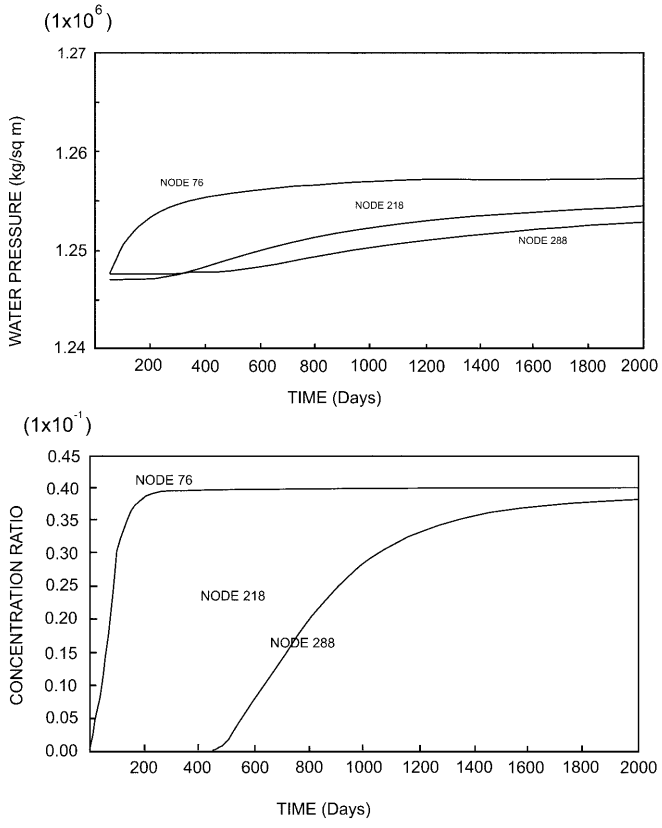

Fig. 15
Temporal change of pressure and concentration at some nodes for α_l=25 m and α_t=1 m and Δt=5 days

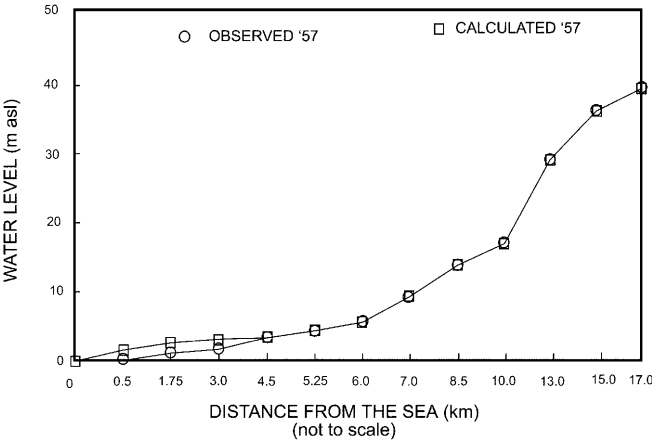

Fig. 16
Comparison of the calibrated model results with the observed water levels in 1957

(Fig. 12), they are averaged among the neighboring elements located along the profile. Calibrated head and concentration values (Fig. 17) were stored to be used as initial values in the transient analysis.

Transient runs

Transient simulation of the aquifer for the 1957–1993 period was performed by conducting simulation runs in the cross sectional model. Calibrated model results were used as the initial values and the modeling was progressed through time to simulate the response of the aquifer to temporal changes in the recharge and discharge conditions. Finally, the calibrated and history-matched model was applied to make future predictions for the saltwater intrusion in the Tripoli region.

Transient modeling utilized the initial conditions obtained during transient steady-state calibration, and progressed through time to make a history match for the period of 1957 to 1993. History matching was performed in two steps because of the presence of different water demand periods. High water demands for increased agricultural and industrial activities, as well as an increased population after 1971, necessitated history matching for two periods: 1957–1971 and 1972–1993. The calibrated parameters, the boundary conditions, and the initial conditions were used in the transient simulation runs.

Previous studies have considered different recharge mechanisms into the aquifer (Pallas 1978; Krummenacher 1982; NCB and MM 1993). Among these mechanisms, recharge from rainfall, recharge from irrigation returns, recharge from south inflow, and even recharge from municipal supply losses are mentioned. Because of these mechanisms, this study assumed percentages of water amounts that recharged the aquifer: 10% rainfall, 30% irrigation discharge, 15% municipal discharge, and south inflow were estimated as the major recharge components. South inflow was evaluated by using the hydraulic

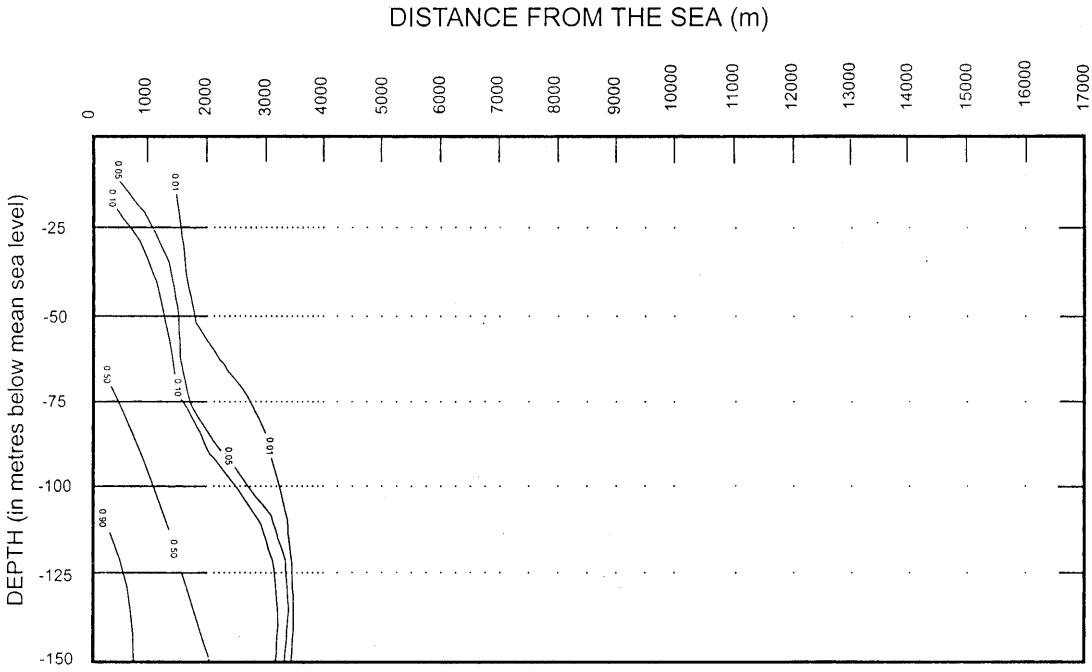

Fig. 17
Steady-state model calculations for the concentration ratios in 1957

gradient, the water levels, and the hydraulic conductivities along the southern boundary. On the other hand, the amount of water withdrawal by pumping wells defined the total discharge from the aquifer. This was defined as the discharge for agricultural and municipality needs.

Because of temporal changes in the recharge and discharge components, an analysis was conducted to determine the amount of net inflow or outflow from the aquifer. This was repeated for each year and annual net flow amounts were computed and input to the simulation. Table 3 lists the discharge and recharge components and the related net inflow/outflow used in the computer runs. Some of these components (discharge for municipality, recharge from rainfall) were available and some (discharge for agriculture, recharge from irrigation returns, recharge from municipality water losses) were estimated.

Distribution of these total discharge and recharge values was accomplished by defining three different zones (Fig. 18) depending on their activity changes during the simulation period (Table 3). In this way, the recharge and discharge components (net inflow/outflow) were evaluated to incorporate the spatial variation as suggested by Anderson and Woessner (1992). The net flow amounts were input into the model using the surface areas of each zone (Table 4). In this consideration, the cross sectional model had a width of 250 m, which was estimated by using the radius of influence of the water wells.

Transient runs calculated the nodal pressures, heads, and the nodal concentrations, and the results are given in Figs. 19 and 20. A very good match was obtained for the first period in terms of the water levels. Comparison of the concentration distributions reveals a slight discrepancy in this period. In other words, the intrusion mechanism was not yet accelerated at that period. Although data were not available, presumably the water demand was not as high in this period. This is also verified by the net flow deficiency amounts listed in Table 4. Negative net flow amounts between 1957 and 1971 increased to three times the amount during 1972–1983 and to more than five times the amount during 1984–1993. Second-step transient simulations correspond to the 1972–1993 period, where water demand accelerated because of increased use of groundwater in the region (Table 4). This has resulted in a remarkable decline in water levels along the profile (Fig. 21). Inevitably, the salt concentrations have increased is reflected in the progressive landward migration of seawater (Fig. 22). Field verification of the concentrations was made by comparing the computed values with those observed during field observations in 1994. Table 5 shows the observed concentrations in nine wells located along the profile. Although it is impossible to make a one-to-one match of the values, the computed values correlate to some extent with the observed con-

Table 3
Temporal change of discharge and recharge parameters in the selected zones

Period	1957–1971		1972–1982		1983–1993	
Zone	Discharge	Recharge	Discharge	Recharge	Discharge	Recharge
ZI	DAGDMN	RRFRAGRMN	DAGDMN	RRFRAGRMN	DAGDMN	RRFRAGRMN
ZII		RRF	DAGDMN	RRFRAGRMN	DAGDMN	RRFRAGRMN
ZIII		RRF		RRF	DAGDMN	RRFRAGRMN

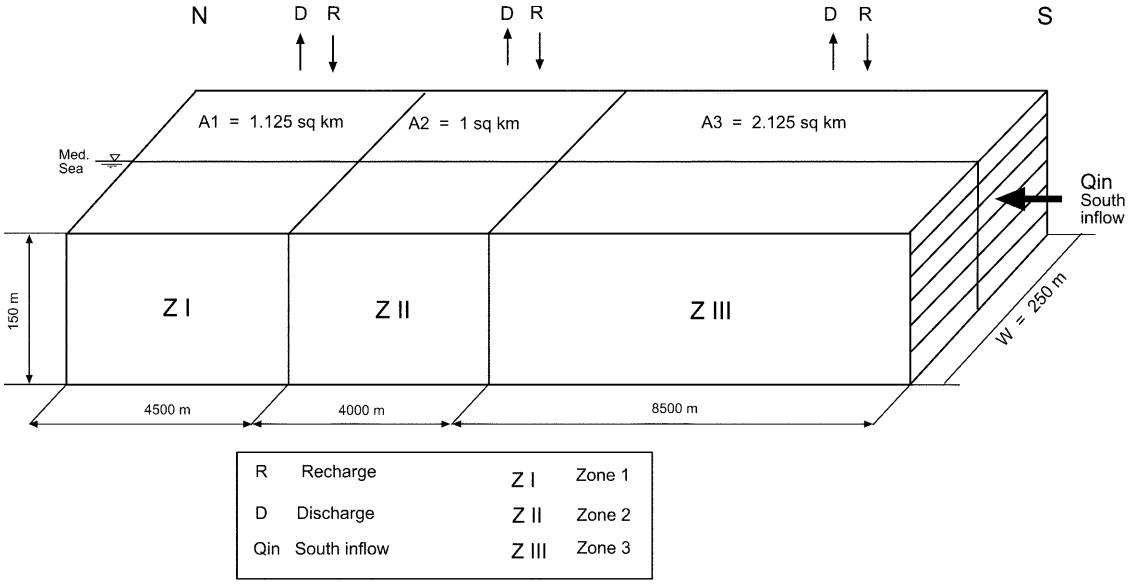

Fig. 18
Schematic representation of the zonation for Gargaresh profile

centrations. Lack of fit for some wells could be explained by inefficiencies of the wells, different production conditions, different depths, etc. On the other hand, computed

Table 4
Discharge and recharge components and the net flows used in transient runs. *DAG* Annual discharge for agriculture (m^3); *DMN* annual discharge for municipality (m^3); *TDIS* total annual discharge (m^3); *RRF* annual recharge from rainfall (m^3); *RAG* annual recharge from irrigation returns (m^3); *RMN* annual recharge from municipality water losses (m^3); *TREC* total annual recharge (m^3)

Year	DAG	DMN	TDIS	RRF	RAG	RMN	TREC	NET
1957	212,500	50,145	262,645	134,225	63,750	7,522	214,497	–48,148
1958	212,500	51,874	264,374	129,625	63,750	7,781	201,156	–63,218
1959	212,500	54,468	266,958	93,500	63,750	8,170	165,420	–101,538
1960	212,500	57,062	269,561	201,025	63,750	8,559	273,334	3,773
1961	212,500	58,790	271,290	119,850	63,750	8,819	192,419	–78,871
1962	212,500	63,113	275,613	92,225	63,750	9,467	165,442	–110,171
1963	212,500	65,707	278,207	151,300	63,750	9,856	224,906	–53,301
1964	212,500	70,025	282,525	105,825	63,750	10,504	180,079	–102,446
1965	212,500	72,969	285,469	76,075	63,750	10,945	150,770	–134,699
1966	212,500	76,082	288,582	158,100	63,750	11,412	233,262	–55,320
1967	212,500	81,615	294,115	88,825	63,750	12,242	164,817	–129,290
1968	212,500	86,457	298,957	63,750	63,750	12,969	140,469	–158,488
1969	212,500	91,644	304,144	125,375	63,750	13,747	202,872	–101,272
1970	212,500	98,560	311,060	96,900	63,750	14,784	175,435	–135,626
1971	212,500	107,898	320,398	147,475	63,750	16,185	227,410	–92,988
1972	425,000	172,141	597,141	152,575	127,500	25,821	305,896	–291,245
1973	425,000	182,511	607,511	170,850	127,500	27,377	325,727	–281,784
1974	425,000	192,363	617,363	141,525	127,500	28,854	297,879	–319,484
1975	425,000	204,807	629,807	229,075	127,500	30,721	387,296	–242,511
1976	425,000	214,140	639,140	83,300	127,500	32,121	242,951	–396,219
1977	425,000	227,621	652,621	132,600	127,500	34,143	294,243	–358,378
1978	425,000	238,509	663,509	221,000	127,500	35,776	384,276	–279,233
1979	425,000	251,472	676,472	119,425	127,500	37,721	284,646	–391,826
1980	425,000	272,211	697,211	182,750	127,500	40,832	351,082	–346,129
1981	425,000	284,655	709,655	114,325	127,500	42,698	284,523	–425,132
1982	425,000	295,544	720,544	149,600	127,500	44,332	321,432	–399,112
1983	562,500	418,450	980,950	164,050	168,750	62,767	395,567	–585,383
1984	562,500	428,825	991,325	179,775	168,750	64,324	412,849	–578,476
1985	562,500	442,658	1,005,158	84,575	168,750	66,399	319,274	–685,434
1986	562,500	453,032	1,015,532	232,900	168,750	67,955	469,605	–545,927
1987	562,500	470,324	1,032,824	130,900	168,750	70,549	370,199	–662,625
1988	562,500	484,157	1,046,657	247,775	168,750	72,624	489,149	–557,508
1989	562,500	498,682	1,061,182	156,825	168,750	74,802	400,377	–660,805
1990	562,500	515,281	1,077,781	155,975	168,750	77,292	402,017	–675,764
1991	562,500	529,114	1,091,614	136,000	168,750	79,367	384,117	–707,497
1992	562,500	553,322	1,115,822	75,650	168,750	82,998	327,398	–788,424
1993	562,500	561,968	1,124,468	99,450	168,750	84,295	352,495	–771,973

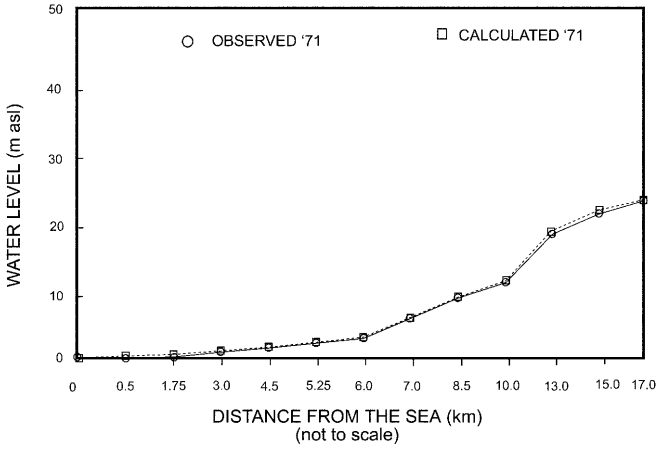

Fig. 19
Comparison of the observed and calculated water levels along the Gargaresh profile in 1971

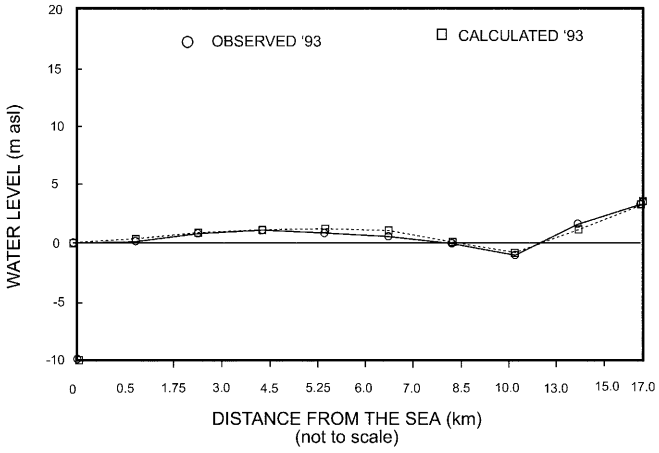

Fig. 21
Comparison of the observed and calculated water levels along the Gargaresh profile in 1993

concentrations successfully verify the surface position of the 375 mg/l contour (Fig. 5). This fact was simulated using the proposed algorithm, and history matching for both the water levels and concentrations was successfully completed.

Calibrated and history matched simulation was applied to the Tripoli region in order to predict the future behavior of the intrusion. In this analysis an average annual rainfall of 310 mm was used. The positive effect of the Great Man Made River Project (NCB and MM 1993), which would import water from the southern region, was also introduced into the predictions. This project plans to supply 400,000 m^3 of water per day, starting in 1996, and 1,000,000 m^3 of water per day after 1999 (NCB and MM 1993). Prediction runs considered these amounts in the computations. Figure 23 shows the position of the concentration ratios along the Gargaresh profile in 2005. It depicts that 0.01 ratio would reach to shallow wells at distances of 5-km from the coast and deeper wells would pump more saline water because of the rising intrusion. It is quite clear that present water production policies need to be modified otherwise the aquifer will be severely contaminated by progressive seawater intrusion.

Conclusions

Numerical research was introduced in this paper to investigate the problem of seawater intrusion into a coastal aquifer along the Mediterranean coast of Libya. Characteristics of the intrusion mechanism and its spatial and temporal variation, as well as its future behavior, were thoroughly investigated by means of a two-step numerical model.

A proposed simulation algorithm required two-step modeling that could be treated as a quasi-three-dimensional approach. First an areal vertical integrated flow model was applied to calibrate the physical parameters for definition of the flow mechanism, and the initial condi-

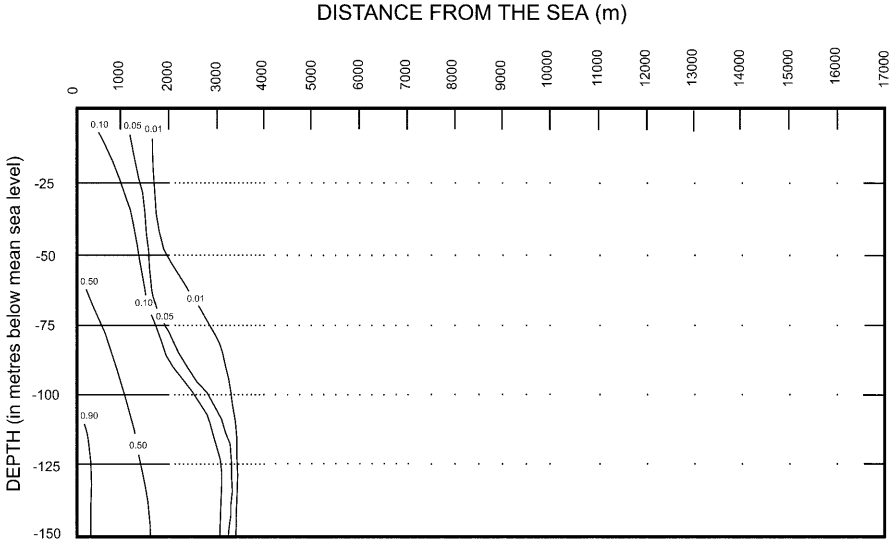

Fig. 20
Distribution of concentration ratios along the Gargaresh profile in 1971

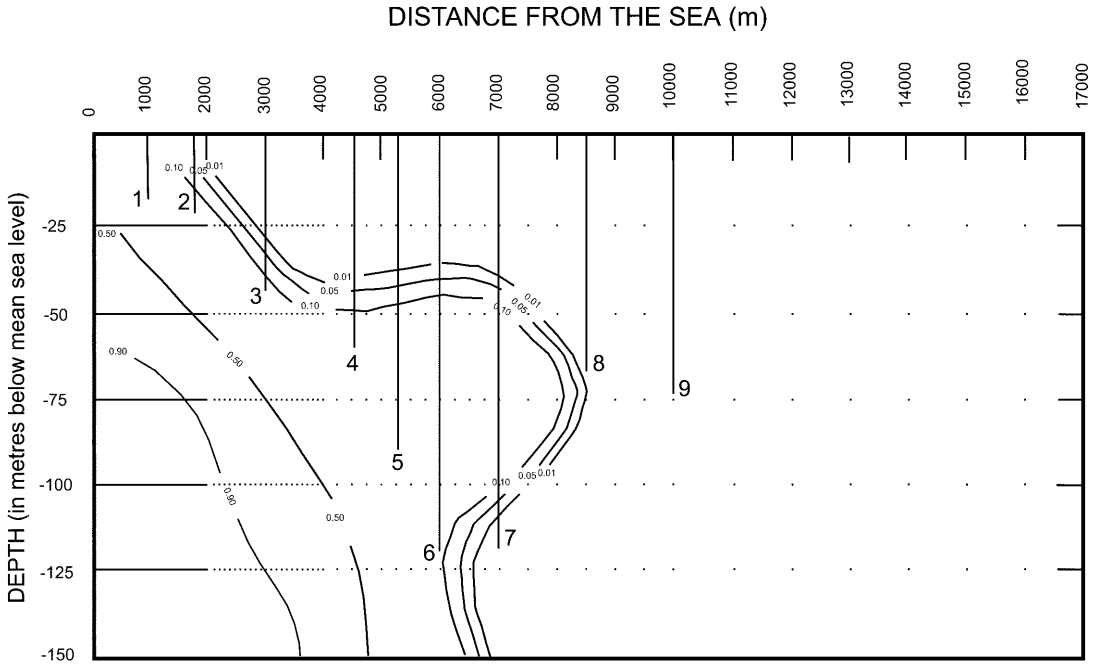

Fig. 22
Distribution of concentration ratios along the Gargaresh profile in 1993

tions for flow were evaluated accordingly. Second, the cross sectional model was utilized to incorporate the diffusion and hydrodynamic dispersion mechanisms into the simulation, and it determined the original equilibrium between the seawater and the freshwater phases via a transient calibration scheme. Afterwards, the simulation

Table 5
Chloride concentrations observed in wells along Gargaresh Profile (1994)

Well no.	Depth (m)	Distance from coast (m)	Concentration of Cl^- (mg/l)
128	20	1,000	860
129	20	1,750	860
130	45	3,000	4,070
131	65	4,500	800
132	90	5,250	1,570
133	120	6,000	4,650
134	120	7,000	9,120
135	68	8,500	100
136	75	10,000	100

Fig. 23
Distribution of concentration ratios along the Gargaresh profile in 2005

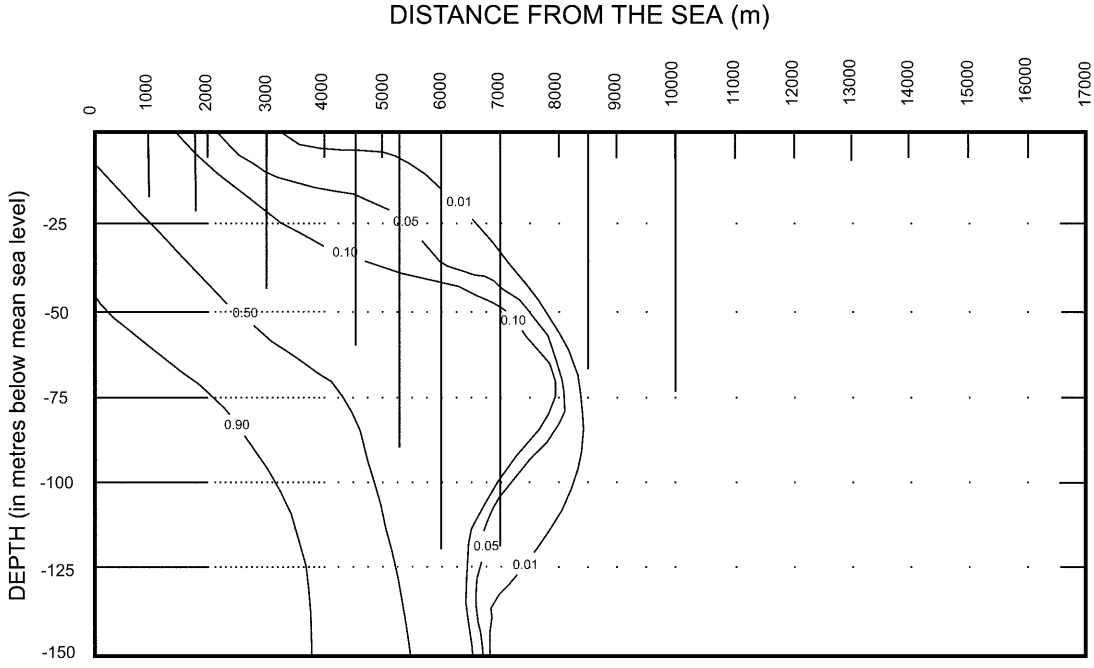

was progressed through time in order to evaluate the aquifer's temporal response to the foregoing conditions. This was accomplished utilizing the coupled behavior of the fresh water flow and the salt transport mechanisms that occur in coastal aquifers.

Steady-state calibrations with data reported for the 1950s and the history matching period 1950–1993 were found to be successful. Physical parameters and recharge values were appropriate to be used in modeling the seawater intrusion in the coastal aquifer of Tripoli. Transient simulations, which started with unpolluted initial conditions, reached a steady-state with respect to well discharge in the 1950s, which could be successfully matched with observed data.

Transient simulation runs have shown that the aquifer in the Tripoli region is over-pumped. Particularly in the last 20 years, too much groundwater has been extracted. Inevitably, this has accelerated seawater intrusion and caused landward migration of the intrusion.

Future predictions clarify that discharge from the aquifer should be properly managed, as this is the only water resource for the region. Migration rate of the intrusion could be reduced by thorough investigation and by planning new management policies for optimal use of the freshwater in the aquifer.

References

Anderson MP, Woessner WW (1992) Applied groundwater modeling, simulation of flow and advective transport. Academic Press, London

Backush IM (1983) A quantitative model of Gefara plain central part NW Libya. MSc Thesis, Ohio University

Bear J, Dagan G (1964) Moving interface in coastal aquifers. J Hydraul Div Am Soc Civil Eng 99(HY4):193–216

Bilal WM (1987) Seawater intrusion in Janzur. BSc Thesis, El Fateh University, Tripoli

Cedestrom D, Bastaiola H (1960) Groundwater in the Tripoli area, Libya. USGS Open File Report

Croucher AE, O'Sullivan MJ (1995) The Henry problem for saltwater intrusion. Water Resour Res 31(7):1809–1814

Emekli N, Karahanoglu N, Yazýcýgil H, Doyuran V (1996) Numerical simulation of saltwater intrusion in a groundwater basin. Water Environ Res 68(5):855–866

Essaid HI (1990) A multilayered sharp interface model of coupled freshwater and saltwater flow in coastal systems: model development and application. Water Resour Res 26(7):1451–1453

FAO (1981) The Gefara plain water management plan. FAO, LIB/005

Floegel H (1979) Seawater intrusion study. SARLD Report, Tripoli

Frind EO (1982) Simulation of long-term transient density-dependent transport in groundwater. Adv Water Resour 5:73–97

GEFLI (1972) Soil and water resources survey for hydro-agricultural development, Western Zone. Unpublished Report, Ground Water Authority, Tripoli

Huyakorn PS, Wu YS, NS Park (1996) Multiple approach to the numerical solution of a sharp interface saltwater intrusion problem. Water Resour Res 32(1):93–102

IRC (1975) Geological map of Libya, 1:250,000 sheet. Tarabulus, explanatory booklet. Industrial Research Center, Tripoli

Krummenacher R (1982) Report on groundwater resources of Gefara plain. SARLD Report, Tripoli

Kruseman GP (1977) Evaluation of water resources of the Gefara plain. SDWR, unpublished report, Tripoli

Kruseman GP, Floegel H (1978) Hydrogeology of the Gefara plain, NW Libya. 2nd Symposium Geology of Libya, Tripoli

Meludi H, Werynski K (1980) Seawater intrusion study, Gargaresh Swani Well Field area. SARLD Report, Tripoli

NCB and MM (1993) Water management plan. Great Man Made River Water Utilization Authority by the National Consulting Bureau of GSPLAJ with Mott MacDonald of the UK, Tripoli

Pallas P (1978) Water resources of the SPLAJ. SDWR, Tripoli

Reilly TE, Goodman A (1985) Quantitative analysis of saltwater-freshwater relationships in groundwater systems, a historical perspective. J Hydrol 80:125–160

Shamir U, Dagan G (1971) Motion of seawater interface in coastal aquifers: a numerical solution. Water Resour Res 7(3):644–657

Shawi T, Philbert M (1991) A study of seawater intrusion in Tajura groundwater. BSc Project, El Fateh University, Tripoli

Voss CI (1984) SUTRA: a finite element simulation model for saturated-unsaturated, fluid density dependent ground-water flow with energy transport or chemically reactive single species solute transport. US Geological Survey Water-Resources Investigations Report 84-4369

Voss CI, Andersson J (1993) Regional flow in the Baltic Shield during Holocene coastal regression. Ground Water 31(6):989–1006

Wilson J, Sa da Costa A (1982) Finite element simulation of a saltwater/freshwater interface with indirect toe tracking. Water Resour Res 18(4):1069–1080

Xue Y, Xie C, Wu J, Liu P, Wang J, Jiang Q (1995) A three dimensional miscible transport model for seawater intrusion in China. Water Resour Res 31(4):903–912